International Journal of Minerals, Metallurgy and Materials
Volume 22, Number 10, October 2015, Page 1092
DOI: 10.1007/s12613-015-1172-1

In situ (α-Al_2O_3+ZrB_2)/Al composites with network distribution fabricated by reaction hot pressing

El Oualid Mokhnache[1)], *Gui-song Wang*[1)], *Lin Geng*[1)], *Kaveendran Balasubramaniam*[1)], *Abdelkhalek Henniche*[1)], *and Noureddine Ramdani*[2)].

1) School of Materials Science and Engineering, Harbin Institute of Technology, Harbin 150001, China
2) Polymer Materials Research Center, Harbin Engineering University, Harbin 150001, China
(Received: 22 February 2015; revised: 23 March 2015; accepted: 27 March 2015)

Abstract: *In situ* (α-Al_2O_3+ZrB_2)/Al composites with network distribution were fabricated using low-energy ball milling and reaction hot pressing. Differential thermal analysis (DTA) was used to study the reaction mechanisms in the Al–ZrO_2–B system. X-ray diffraction (XRD) and scanning electron microscopy (SEM) in conjunction with energy-dispersive X-ray spectroscopy (EDX) were used to investigate the composite phases, morphology, and microstructure of the composites. The effect of matrix network size on the microstructure and mechanical properties was investigated. The results show that the optimum sintering parameters to complete reactions in the Al–ZrO_2–B system are 850°C and 60 min. *In situ*-synthesized α-Al_2O_3 and ZrB_2 particles are dispersed uniformly around Al particles, forming a network microstructure; the diameters of the α-Al_2O_3 and ZrB_2 particles are approximately 1–3 μm. When the size of Al powder increases from 60–110 μm to 150–300 μm, the overall surface contact between Al powders and reactants decreases, thereby increasing the local volume fraction of reinforcements from 12% to 21%. This increase of the local volume leads to a significant increase in microhardness of the *in situ* (α-Al_2O_3–ZrB_2)/Al composites from Hv 163 to Hv 251.

Keywords: metal matrix composites; network distribution; sintering; hot pressing; microhardness

1. Introduction

The application of discontinuously reinforced aluminum composites (DRAMCs) has attracted the significant attention in the aerospace, automobile, and weapons industries [1–3] because of their good mechanical, thermal, and physical properties. Moreover, DRAMCs fabricated by *in situ* methods have attracted much interest [1–2,4–7] because of their isotropic properties and low cost. Furthermore, Al_2O_3 and ZrB_2 synthesized by *in situ* reactions have been demonstrated to be an effective reinforcement for the Al matrix [5–6]. The mechanical properties of DRAMCs are not only determined by the volume fraction, morphology, and type of reinforcement and matrix, but are also affected by the distribution of the reinforcement material and the morphology of the matrix. The strengthening effect of reinforcement and the ductility effect of the matrix can be better exploited by creating a network reinforcement architecture [7–8].

Some efforts have been made to create the composite materials with a variety of new microstructures that offer the enhanced properties [9–12]. Peng *et al.* [11–12] fabricated the bicontinuous aluminum matrix composites by squeeze casting, where the reinforcement materials formed a network rather than being dispersed in a homogeneous manner. In fact, this network microstructure is based on the famous Hashin–Shtrikman (H–S) bounds theory, which is used to estimate the mechanical properties of quasi-isotropic and quasi-homogeneous multiphase materials. Although the H–S bounds are sufficiently close to provide a good estimate for the effective elastic properties of the conventional composites with arbitrary phase geometry, the upper (lower) bound rigorously corresponds to the composites containing spherical inclusions as a matrix (reinforcement) encapsulated by a reinforcement (matrix) phase [13].

Corresponding author: Gui-song Wang E-mail: wangguisong@hit.edu.cn

Because of the formation of large pores during the *in situ* processing of composites, the reaction hot pressing (RHP) has been proposed as a method to overcome this problem. This method includes the compaction of reaction products after *in situ* synthesis of reinforcements in the matrix to obtain a near fully dense composite [6–7,14].

Recently, extensive research has been devoted to the fabrication of *in situ* (α-Al_2O_3+ZrB_2)/Al composites with the homogeneous microstructures [6,15–16]. Hence, the comparative mechanical properties, such as tensile properties and wear resistance, have been obtained. Furthermore, B/ZrO_2 with the molar ratio of 2 has been reported to completely prevent the formation of Al_3Zr from the Al–ZrO_2–B system, thereby resulting in the formation of only Al_2O_3 and ZrB_2 as reinforcement materials [16]. In fact, Al_3Zr is a very brittle phase, which limits the applications of such composites. On the basis of these previous results, a B/ZrO_2 with the molar ratio of 2 was used in the present study to fabricate dense *in situ* (α-Al_2O_3–ZrB_2)/Al composites with a network structure. Moreover, the influence of Al matrix particle size on the microstructure and mechanical properties of the *in situ* (α-Al_2O_3+ZrB_2)/Al composites was studied. Differential thermal analysis (DTA) was used to determine the reinforcement synthesis temperature in the Al–ZrO_2–B system.

2. Experimental

Pure Al powder with different particle sizes of approximately 60–110, 110–150, and 150–300 μm as well as ZrO_2 (0.5–1 μm) and B (~1 μm) powders were used as the starting materials to produce the *in situ* (α-Al_2O_3+ZrB_2)/Al composites with a network structure; these composites were labeled as C1, C2, and C3, respectively. First, the stoichiometric starting materials were weighed according to the hypothetical reaction. To maintain the spherical design of the network structure, the powder mixtures were ball milled at 125 r/min for 1 h in a planetary ball mill; the powders were milled under an argon atmosphere, and the milling media/material ratio was 4:1. The mixed powders were transferred into a graphite mold pre-coated with boron nitride to avoid reaction between the mold and reactants. Under a vacuum of 4.5×10^{-2} Pa, different stages were used to fabricate the *in situ* (α-Al_2O_3+ZrB_2)/Al composites. In the first stage, the powders were heated to 600°C and compacted at 25 MPa for 1 h to produce the as-sintered (ZrO_2+B)/Al billet with a diameter of 60 mm and a height of 25 mm, thereby enhancing the reactivity in the Al–ZrO_2–B system.

To determine the synthesis temperature of the Al–ZrO_2–B system, a sample with 2 mm in diameter and 1 mm in height cut from the as-sintered (ZrO_2+B)/Al billet was subjected to DTA testing. The sample was heated under an argon atmosphere in a TGA/SDTA85IE thermal analyzer, where the temperature was increased from room temperature (25°C) to 1000°C at a heating rate of 10°C·min^{-1}. After being subjected to DTA, the as-sintered (ZrO_2+B)/Al billet was cut into small samples and each sample was placed into a quartz container that was subsequently evacuated to avoid the oxidation of sample. Subsequently, all samples were heated in a conventional furnace at 850°C for different holding times of 30, 60, and 90 min to produce the composites labeled as C30, C60, and C90, respectively. After the optimum sintering parameters (i.e., the synthesis temperature and holding time) were determined, the *in situ* (α-Al_2O_3+ZrB_2)/Al composites were cooled from 850°C to 600°C and re-compacted at 25 MPa for 1 h to produce the dense composites labeled S60, S110, and S150, respectively, with different Al matrix particle sizes. The raw materials and fabrication process of composites are shown in Fig. 1. All the sintered composites and their sintering parameters are shown in Table 1.

The composite phases were identified using X-ray diffraction (XRD); a Philips X'pert diffractometer was used in the experiments and was equipped with a Cu K_α radiation source. Scanning electron microscopy (SEM, Quanta 200FEG) along with energy-dispersive X-ray spectroscopy (EDX) was used to investigate the microstructure and morphology of the composites. Microhardness measurements were performed on samples using an HVS-1000 Vickers hardness tester.

3. Results and discussion

3.1. Thermodynamic analysis

The variation of Gibbs free energy ($\Delta G_T^\ominus$) can be written as

$$\Delta G_T^\ominus = \Delta H_{298}^\ominus - T\Delta S_{298}^\ominus . \quad (1)$$

where $\Delta H_{298}^\ominus$ and $\Delta S_{298}^\ominus$ are the standard enthalpy and standard entropy, respectively, at room temperature. According to the published thermodynamic data [17], the possible reactions and their accompanying free-energy changes in the Al–ZrO_2–B system can be written as the following equations.

$$4Al + 3ZrO_2 \rightarrow 2Al_2O_3 + 3[Zr] \quad (2)$$

$$\Delta G_T^\ominus = 176603 + 54.63T \quad (3)$$

$$Al + 2B \rightarrow AlB_2 \quad (4)$$

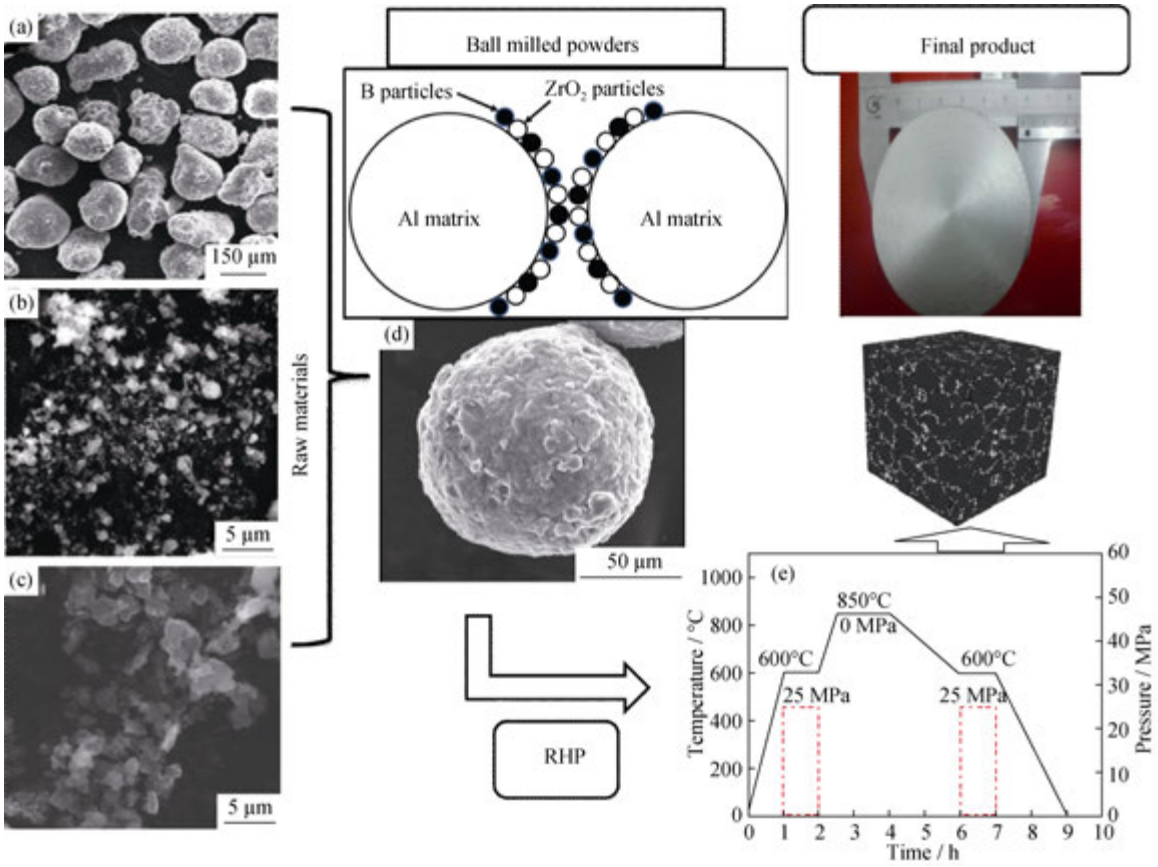

Fig. 1. Raw materials and fabrication process of the composites: (a) Al; (b) ZrO_2; (c) B; (d) ball-milled Al powders; (e) reaction hot pressing parameters.

Table 1. Composite nomenclature and the corresponding sintering parameters

Composite reinforcement phase content = 5vol%	Step 1	Step 2	Step 3
As-sintered (ZrO_2+B)/Al	600°C, 1 h, 25 MPa	none	none
C30	600°C, 1 h, 25 MPa	850°C, 30 min, 0 MPa	none
C60	600°C, 1 h, 25 MPa	850°C, 60 min, 0 MPa	none
C90	600°C, 1 h, 25 MPa	850°C, 90 min, 0 MPa	none
S60 (Al size: 60–110 μm)	600°C, 1 h, 25 MPa	850°C, 60 min, 0 MPa	600°C, 60 min, 25 MPa
S110 (Al size: 110–150 μm)	600°C, 1 h, 25 MPa	850°C, 60 min, 0 MPa	600°C, 60 min, 25 MPa
S150 (Al size: 150–300 μm)	600°C, 1 h, 25 MPa	850°C, 60 min, 0 MPa	600°C, 60 min, 25 MPa

$$\Delta G_T^{\ominus} = -65557 - 5.47T \quad (5)$$

$$3Al + [Zr] \rightarrow Al_3Zr \quad (6)$$

$$\Delta G_T^{\ominus} = -251383 + 319.4T \quad (7)$$

$$AlB_2 + [Zr] \rightarrow ZrB_2 + Al \quad (8)$$

$$\Delta G_T^{\ominus} = -254330 + 41.4T \quad (9)$$

where [Zr] stands for the free Zr which can react either with Al to produce Al_3Zr or with B to produce ZrB_2 as final phases.

According to the study of Zhu *et al*. [6], Eqs. (2), (4), (6), and (8) are thermodynamically feasible and spontaneous. Moreover, three exothermic reactions can occur, leading to three different final products.

$$13Al + 3ZrO_2 \rightarrow 2Al_2O_3 + 3Al_3Zr \ (B/ZrO_2 \text{ by molar} = 0) \quad (10)$$

$$17Al + 6ZrO_2 + 6B \rightarrow 4Al_2O_3 + 3Al_3Zr + 3ZrB_2 \ (B/ZrO_2 \text{ by molar} = 1) \quad (11)$$

$$4Al + 3ZrO_2 + 6B \rightarrow 2Al_2O_3 + 3ZrB_2 \ (B/ZrO_2 \text{ by molar} = 2) \quad (12)$$

According to the Al–Zr phase diagram [18], the intermetallic Al_3Zr is formed through peritectic reaction and congruent melting. However, the brittleness of Al_3Zr is a shortcoming that precludes its practical use as a structural material.

In the present work, because the presence of brittle Al_3Zr phase in the composites was deleterious, a B/ZrO_2 molar ratio of 2 was selected to synthesize only Al_2O_3 and ZrB_2 as new reinforcement materials. In addition, the variation of Gibbs free energy with the temperature of Eq. (12) was negative within the experimental temperature, suggesting that the *in situ* formation of Al_2O_3 and ZrB_2 via Eq. (12) was thermodynamically feasible.

Fig. 2 shows the DTA curve of the as-sintered (ZrO_2+B)/Al composite. A large endothermic peak is observed at 664°C, which is attributable to the energy absorbed by the relatively large volume faction of Al during heating; i.e., the endothermic peak at 664°C corresponds to the melting temperature of aluminum. After the aluminum melts, the reactions in the Al–ZrO_2–B system become more favorable because of the increased elemental diffusion in the Al–Zr–O–B system resulting from the increase in temperature. Therefore, two exothermic peaks at approximately 750°C and 850°C are observed. Consistent with the aforementioned thermodynamics considerations, the first exothermic peak at 750°C corresponds to the reaction between Al and B via Eq. (2), which results in the formation of AlB_2 phase. Subsequently, because of the increase in temperature from 750°C to 850°C, ZrO_2 reacts with Al via Eq. (1), forming Al_2O_3 and Zr. Meanwhile, the free Zr reacts with AlB_2 via Eq. (8), forming ZrB_2 and Al. Consequently, the second exothermic peak at 850°C is a superimposition of two peaks that correspond to Eqs. (1) and (8), which result in the formation of Al_2O_3 and ZrB_2 at the final stage. Notably, the presence of excess boron (B/ZrO_2 = 2) increases the diffusivity of B into Al in comparison to that of Zr into Al, thereby increasing the surface interaction between Zr and B. Consequently, ZrB_2 is more likely to form than Al_3Zr.

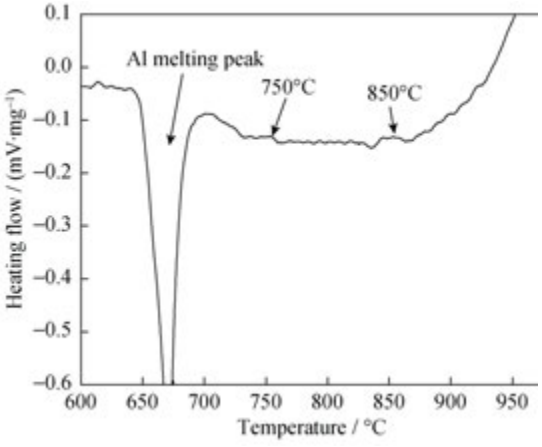

Fig. 2. DTA curve of the as-sintered (ZrO_2+B)/Al composite.

3.2. XRD and microstructures

Fig. 3 shows a typical XRD pattern of the *in situ* (α-Al_2O_3+ZrB_2)/Al composite fabricated in the Al–ZrO_2–B system using a B/ZrO_2 molar ratio of 2. As evident in the figure, three phases, α-Al_2O_3, ZrB_2, and Al, are detected as the final products, whereas neither ZrO_2 nor B is detected. These results suggest that the reactions in Al–ZrO_2–B system occurred completely when the synthesis temperature was 850°C. In addition, Al_3Zr was not present in the *in situ* (α-Al_2O_3+ZrB_2)/Al composite. Therefore, when a B/ZrO_2 molar ratio of 2 was used, the material design of the *in situ* (α-Al_2O_3+ZrB_2)/Al composite was similar to that reported by Zhu *et al.* [6].

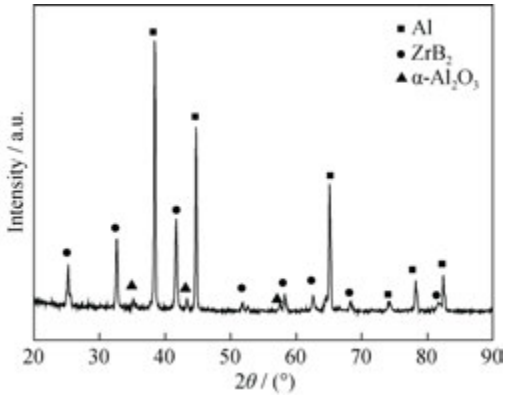

Fig. 3. XRD results for the *in situ* (α-Al_2O_3+ZrB_2)/Al composite (B/ZrO_2 molar ratio = 2).

Figs. 4(a)–(f) show low- and high-magnification SEM images of composites C30, C60, and C90 sintered at 850°C for different holding times of 30, 60, and 90 min, respectively. In the case of composite C30, a portion of the *in situ* reinforcements are dispersed along the Al particle boundaries; however, some Al particles are interpenetrated, indicating that the reactions in Al–ZrO_2–B system do not proceed to the completion at these regions (Figs. 4(a)–(b)). Therefore, a holding time of 30 min is not sufficient for the completion of the reactions between Al, ZrO_2, and B. In the case of composite C60, all reinforcements are dispersed uniformly at Al particle boundaries, suggesting that a holding time of 60 min is sufficient for completion of the reactions in the Al–ZrO_2–B system (Figs. 4(c)–(d)). In fact, sufficient energy to complete the *in situ* reactions depends only on the increase in temperature, as reported in our previous work [4]. However, the use of an extended reaction time can also lead to the growth of Al_3Zr, as observed in the case of composite C90 (Figs. 4(e)–(f)). The growth phenomenon of Al_3Zr was also previously reported in Ref. [19], and the holding time was observed to play a key role in determining the final morphology of Al_3Zr. Consequently, the optimum sintering parameters (i.e., synthesis temperature and holding time) for the fabrication of *in situ* (α-Al_2O_3+ZrB_2)/Al

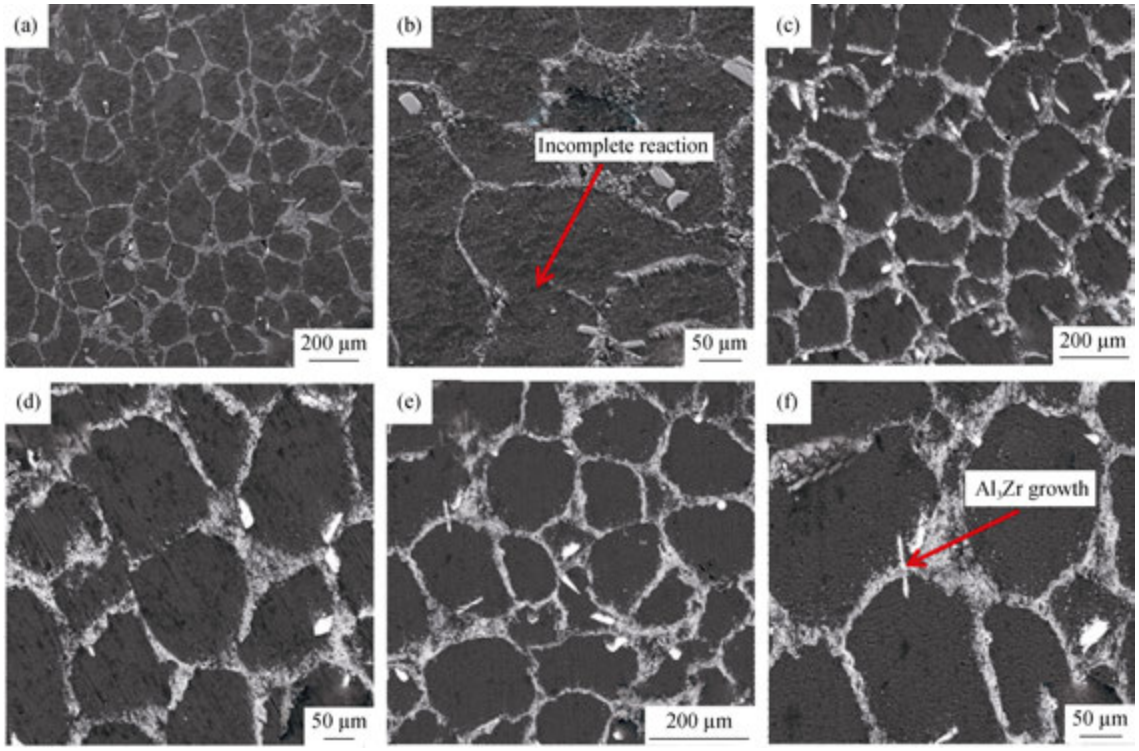

Fig. 4. SEM images of composites sintered at 850°C for different holding times: (a) and (b) 30 min; (c) and (d) 60 min; (e) and (f) 90 min.

composites were determined to be 850°C and 60 min, respectively. Furthermore, because no pressure was applied in the case of composites C30, C60, and C90, large pores were present.

Fig. 5 shows the SEM images and EDX results of the *in situ* (α-Al_2O_3+ZrB_2)/Al composite compacted under a pressure of 25 MPa. As evident in the figure, the size of Al network matrix (~130 μm) is consistent with the size of the ball-milled Al particles, with no interpenetration between the reinforcements and Al matrix; this arrangement may enhance the plasticity of composite. Hence, the final pressing step prevents the formation of pores, thereby resulting in dense composites (Figs. 5(a)–(b)). Furthermore, the *in situ* synthesized α-Al_2O_3 and ZrB_2 particles are dispersed uniformly at the edge of the spherical Al particles (reinforcement rich region), and their sizes are approximately 1–3 μm (Figs. 5(c)–(d)). The EDX results further confirm that these *in situ* reinforcements are Al_2O_3 (the EDX spectrum of point A in Fig. 5(d)) and ZrB_2 (the EDX spectrum of point B in Fig. 5(d)).

3.3. Effect of Al network size

SEM images of the fabricated composites S60, S110, and S150 were used to determine the local volume fraction (V_L) quantitatively, thereby enabling an analysis of the effect of Al particle size on both the final architecture of composites and the enhancement of their mechanical properties. The SEM images of the fabricated composites in Fig. 6 reveal that the network architecture of composites is divisible into two parts (phases I and II): the enhanced rich *in situ* reinforcing area (phase I) and the matrix region (II). Because the Al matrix particles are still assumed to be spherical, the local volume fraction of reinforcements ((α-Al_2O_3+ZrB_2) rich region) can be determined by measuring the width of the reinforcement-rich area, and V_L can be calculated using the following equation.

$$V_L = \frac{\frac{4}{3}\pi\left(\frac{D}{2}\right)^3 \cdot V_C}{\frac{4}{3}\pi\left(\frac{D}{2}\right)^3 - \frac{4}{3}\pi\left(\frac{D}{2}-d\right)^3} \tag{13}$$

where V_L is the local volume fractions of reinforcements, V_C the overall volume fraction of reinforcements, D the average particle size, and d the interface width. V_L for different Al matrix particle sizes was calculated via Eq. (13); the results are summarized in Table 2.

As evident from the results in Table 2, the local volume fraction is increased from 12% to 21% when the Al particle size is increased from 60–110 to 150–300 μm. This result is in accordance with the SEM images in Figs. 6(b)–(c). When the local volume fraction of reinforcement is relatively high, a wall-like ceramic reinforcement network is formed; i.e.,

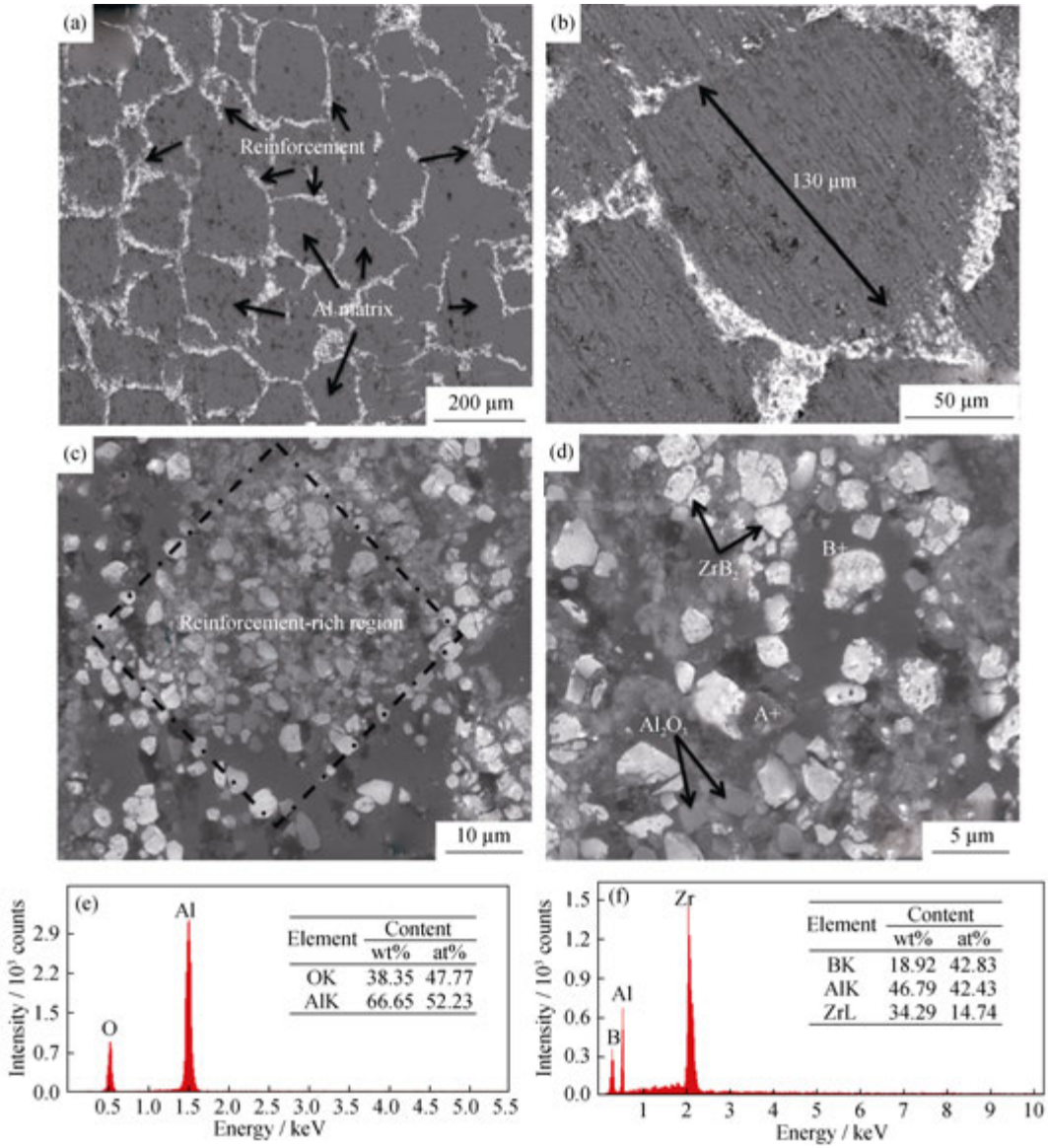

Fig. 5. SEM images and EDX results of the *in situ* (α-Al_2O_3+ZrB_2)/Al composite compacted under a pressure of 25 MPa: (a) and (b) SEM images of composite S110 with a network structure; (c) and (d) SEM images of the reinforcements' aggregation at Al grains; (e) EDX spectrum collected at point A in (d); (f) EDX spectrum collected at point B in (d).

with the increase of Al particle size, the overall surface contact decreases and the local reinforcement content gradually increases. This behavior is attributed to the inner layer of ZrO_2 and B, which is in direct contact with the Al matrix, first reacting to form α-Al_2O_3 and ZrB_2 phases, thereby generating an inner barrier that limits the ability of the outer layer of ZrO_2 and B to react with Al. In this case, only the diffusion of Al through the interface can lead to the generation of α-Al_2O_3 and ZrB_2 at the outer layer. This process is illustrated in Fig. 7 to show the effect of the particle size on the local volume fraction. This illustration shows that the decrease of the overall surface as a consequence of the increase in Al particle size decreases the direct contact between both the ZrO_2 and B particles in one side and the Al from the other side, thereby generating a large amount of reinforcements by diffusion from the inner layer to the outer layer.

3.4. Hardness measurements

Fig. 8 shows the results of Vickers microhardness measurements at different positions for composites S1, S2, and S3 fabricated with Al matrix particle sizes of 60–110, 110–150, and 150–300 μm, respectively. Notably, the microhardness measurements are an average of three readings taken at a particular region. Moreover, when the microhardness values of composites S60, S110, and S150 at position 1 are compared, no obvious variations of the microhardness with respect to the basic area of the network structure are observed.

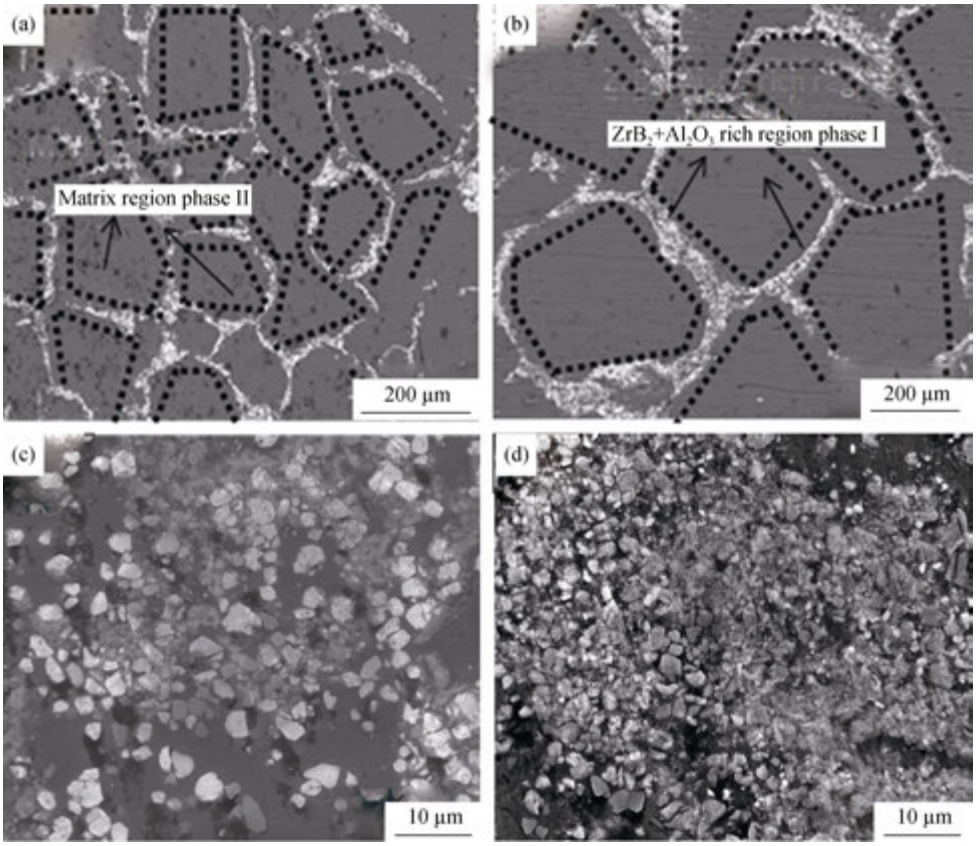

Fig. 6. SEM images of composites: (a) and (c) S1; (b) and (d) S3.

Table 2. Local volume fractions with different Al particle sizes of the *in situ* (α-Al_2O_3+ ZrB_2)/Al composites

Al particle size, D / μm	Overall volume fraction, V_C / %	Interface width, d / μm	Local volume fraction, V_L / %
60–110	5	7	12
110–150	5	8.5	15
150–300	5	10	21

However, at positions 2 and 3, a significant increase in microhardness is observed when the particle size is increased from 60–110 to 150–300 μm. In addition, the microhardness of the *in situ* (α-Al_2O_3+ZrB_2)/Al composite at position 3 is higher than that at position 2, which is attributable to the wall-like ceramic structure caused by the increase in the local volume fraction of reinforcements in this region. As previously mentioned, increasing the Al particle size from 60–110 to 150–300 μm led to an increase of the locally rich reinforcement regions at the edge of the Al matrix, thereby increasing the hardness from Hv 109 to Hv 157 and from Hv 163 to Hv 251 at positions 2 and 3, respectively.

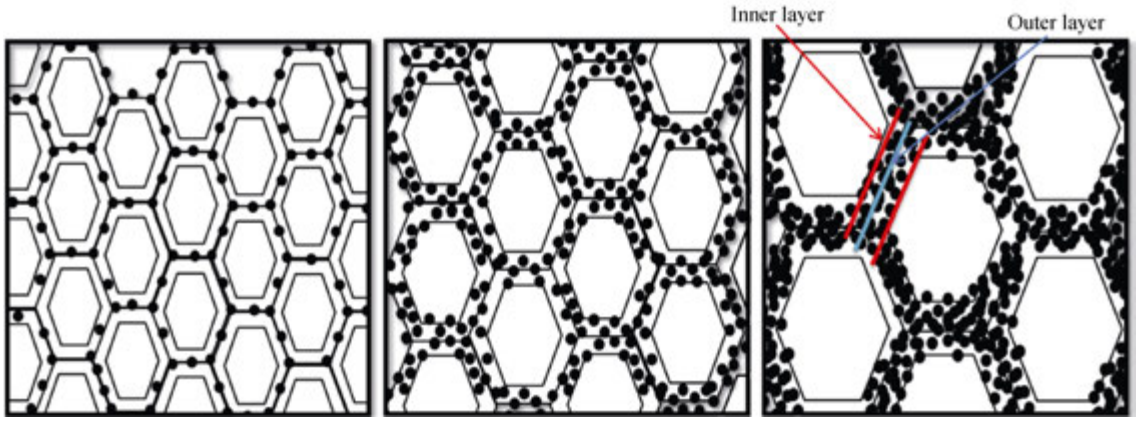

Fig. 7. Schematic showing the effect of increasing Al particle size on increasing the local volume fraction of reinforcements.

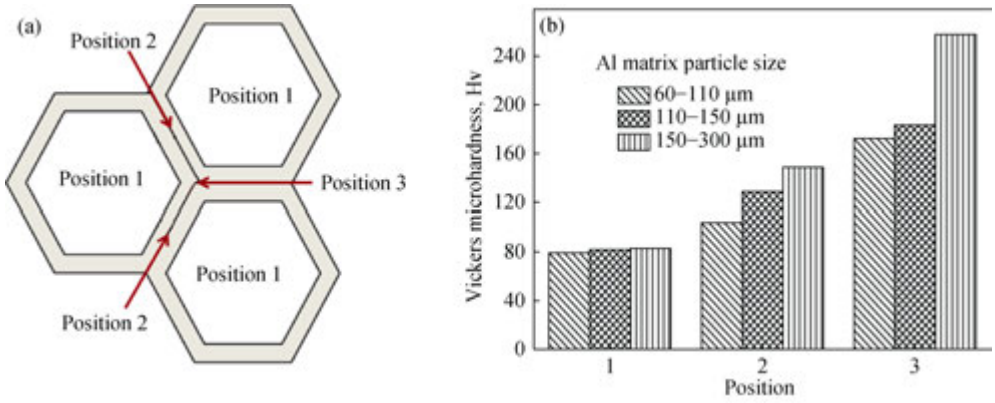

Fig. 8. Schematic of Vickers microhardness measurement (a) and Vickers microhardness vs. Al matrix particle size at different positions (b).

4. Conclusions

(1) *In situ* (α-Al_2O_3+ZrB_2)/Al composites with network distribution are successfully fabricated via reaction sintering. The optimum sintering parameters for the completion of reactions in the Al–ZrO_2–B system are determined to be 850°C and 60 min.

(2) When the Al matrix particle size increases from 60–110 to 150–300 μm, the overall surface decreases, thereby increasing the local volume fraction of reinforcements from 12% to 21%.

(3) The microhardness of the composites increases with increasing Al particle size because of the large local volume fraction of *in-situ* synthesized α-Al_2O_3 and ZrB_2 particles at the Al particle boundaries.

Acknowledgement

This work was financially supported by the National Natural Science Foundation of China (No. 51201047), the Major State Basic Research Development Program of China (No. 2012CB619600), the China Postdoctoral Science Foundation (No. 20110491038), and the Fundamental Research Funds for the Central Universities of China (No. HIT.NSRIF.2013001).

References

[1] S.C. Tjong and Z.Y. Ma, Microstructural and mechanical characteristics of *in situ* metal matrix composites, *Mater. Sci. Eng. R*, 29(2000), No. 3-4, p. 49.

[2] Z.Y. Ma and S.C. Tjong, *In situ* ceramic particle-reinforced aluminum matrix composites fabricated by reaction pressing in the TiO_2(Ti)–Al–B (B_2O_3) systems, *Metall. Mater. Trans. A*, 28(1997), No. 9, p. 1931.

[3] X.H. Qu, L. Zhang, M. Wu, and S.B. Ren, Review of metal matrix composites with high thermal conductivity for thermal management applications, *Prog. Nat. Sci. Mater. Int.*, 21(2011), No. 3, p. 189.

[4] E.O. Mokhnache, G.S. Wang, L. Geng, B. Kaveendran, and L.J. Huang, Synthesis and characterization of *in situ* (Al_2O_3–Si)/Al composites by reaction hot pressing, *Acta Metall. Sin. Engl. Lett.*, 27(2014), No. 5, p. 930.

[5] H.G. Zhu, J. Min, J.L. Li, Y.L. Ai, L.Q. Ge, and H.Z. Wang, *In situ* fabrication of (α-Al_2O_3+Al_3Zr)/Al composites in an Al–ZrO_2 system, *Compos. Sci. Technol.*, 70(2010), No. 15, p. 2183.

[6] H.G. Zhu, J. Min, J.L. Li, J. Chen, J. Zhao, and Y.Q. Yao, Influence of B/ZrO_2 molar ratios on the ambient temperature wear properties of composites made by an Al–ZrO_2–B system, *Wear.*, 271(2011), No. 5-6, p. 635.

[7] L.J. Huang, L. Geng, A.B. Li, F.Y. Yang, and H.X. Peng, *In situ* TiBw/Ti–6Al–4V composites with novel reinforcement architecture fabricated by reaction hot pressing, *Scripta Mater.*, 60(2009), No. 11, p. 996.

[8] L.J. Huang, L. Geng, and H.X. Peng, *In situ* (TiBw+TiCp)/Ti6Al4V composites with a network reinforcement distribution, *Mater. Sci. Eng. A*, 527(2010), No. 24-25, p. 6723.

[9] L.J. Huang, L. Geng, and H.X. Peng, Microstructurally inhomogeneous composites: is a homogeneous reinforcement distribution optimal? *Prog. Mater. Sci.*, 71(2015), p. 93.

[10] H.X. Peng, Z. Fan, J.R.G. Evans, and J.J.C. Busfield, Microstructure of ceramic foams, *J. Eur. Ceram. Soc.*, 20(2000), No. 7, p. 807.

[11] H.X. Peng, Z. Fan, and J.R.G. Evans, Bi-continuous metal matrix composites, *Mater. Sci. Eng. A*, 303(2001), No. 1-2, p. 37.

[12] H.X. Peng, Z. Fan, and J.R.G. Evans, Novel MMC microstructures prepared by melt infiltration of reticulated ceramic preforms, *Mater. Sci. Technol.*, 16(2000), No. 7-8, p. 903.

[13] Z. Hashin and S. Shtrikman, A variational approach to the theory of the elastic behaviour of multiphase materials, *J.*

Mech. Phys. Solids, 11(1963), No. 2, p. 127.

[14] E.O. Mokhnache, G.S. Wang, L. Geng, and L.J. Huang, Microstructures and mechanical properties of *in situ* Al_2O_3/Al–Si composites fabricated by reaction hot pressing, *Metall. Mater. Trans. B*, 45(2014), No. 6, p. 1965.

[15] H.G. Zhu, C.C. Jia, J.L. Li, J. Zhao, J.Z. Song, Y.Q. Yao, and Z.H. Xie, Microstructure and high temperature wear of the aluminum matrix composites fabricated by reaction from Al–ZrO_2–B elemental powders, *Powder Technol.*, 217(2012), p. 401.

[16] H.G. Zhu, Y.Q. Yao, J.L. Li, S. Chen, J. Zhao, and H.Z. Wang, Study on the reaction mechanism and mechanical properties of aluminum matrix composites fabricated in an Al–ZrO_2–B system, *Mater. Chem. Phys*, 127(2011), No. 1-2, p. 179.

[17] O.V. Dorofeeva, V.S. Iorish, V.P. Novikov, and D.B. Neumann, NIST-JANAF thermochemical tables. II. Three molecules related to atmospheric chemistry: HNO_3, H_2SO_4, and H_2O_2, *J. Phys. Chem. Ref. Data*, 32(2003), No. 2, p. 879.

[18] H. Okamoto, Al–Zr (aluminium–zirconium), *J. Phase Equilib.*, 23(2002), No. 2-4, p. 455.

[19] B. Kaveendran, G.S. Wang, L.J. Huang, L. Geng, and H.X. Peng, *In situ* (Al_3Zr+Al_2O_3np)/2024Al metal matrix composite with novel reinforcement distributions fabricated by reaction hot pressing, *J. Alloys Compd.*, 581(2013), p. 16.